

Supporting Information

Anesthetic modulation of protein dynamics: insights from a NMR study

Christian G. Canlas, Tanxing Cui, Ling Li, Yan Xu, Pei Tang*

Table of Contents:

I. Effect of detergent ratio on mistic	S2
II. Calculation of K_d	S2
III. Mistic structure refinement using RDC	S2-S3
IV. ^{15}N R_1 , R_2 , NOE data	S3
V. Residues having conformational exchange	S4
RDC data table	S5-S7
Reference	S7

I. The residues sensitive to changes of the micelle head-groups are likely located in micelle-water interface.

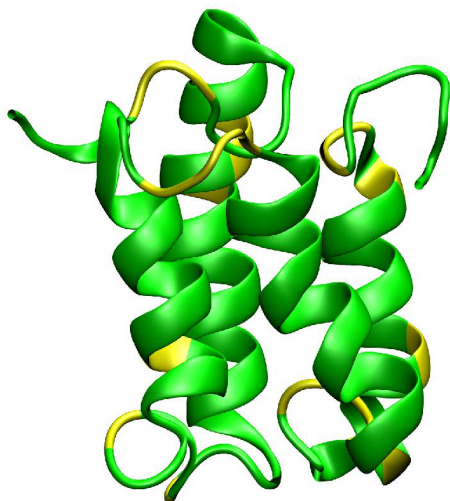


Figure 1S. The residues highlighted in yellow had large change in their chemical shift when the detergent composition was changed from 100% DPC to 40%LDAO/ 60%DPC, suggesting that these residues are located close to the micelle head-groups.

II. Estimation of halothane dissociation constants in Mystic based on changes of residues ^1H - ^{15}N chemical shifts as a function of halothane concentrations.

The residue-specific dissociation constants, K_d , were obtained from the plot of (1):

$$\frac{1}{\Delta\delta} = \left(\frac{1}{\Delta\delta_{\max}} \right) + \left(\frac{K_d}{\Delta\delta_{\max}} \right) \frac{1}{[A_0]} \quad [\text{Eq. S1}]$$

Where $\Delta\delta$ is the change of chemical shift in Hz, $[A_0]$ is halothane concentration in mM, and $\Delta\delta_{\max}$ is the maximum chemical shift difference between halothane in free and in hypothetically fully bound to Mystic.

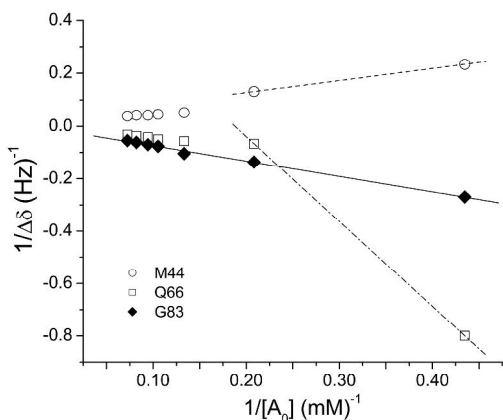


Figure 2S. The reciprocal chemical shift changes vs. the reciprocal halothane concentrations on three representative residues. The slope and intercept of each fitted line give an apparent dissociation constant, K_d , on the basis of **Eq. S1**.

Residues M44 and Q66 show greater or smaller slope at lower or higher halothane concentrations, respectively, indicating that these residues reside at the sites of Mystic where halothane has a limited access and interaction capacity. The derived K_d values for M44, Q66, and G83 are 5, 3, and 26 mM, correspondingly.

III. Structural Refinement using RDC

Figure 3S-A shows good correlations between the experimental RDC values and the back-calculated RDCs of refined structures of Mystic in DPC. Comparison of the refined structure in DPC with the published structure in LDAO constitutes an average backbone root

mean square deviation (RMSD) of 1.3 Angstrom, suggesting that Mystic folds similarly in LDAO and DPC.

A good correlation between the experimental RDCs and the back-calculated RDCs from refined Mystic structure in the presence of halothane is shown in Figure 3S-B. Mystic structures refined using RDC constraints in the absence and presence of halothane showed backbone RMSD of 0.6 Angstrom, suggesting minimal halothane effect on Mystic structures.

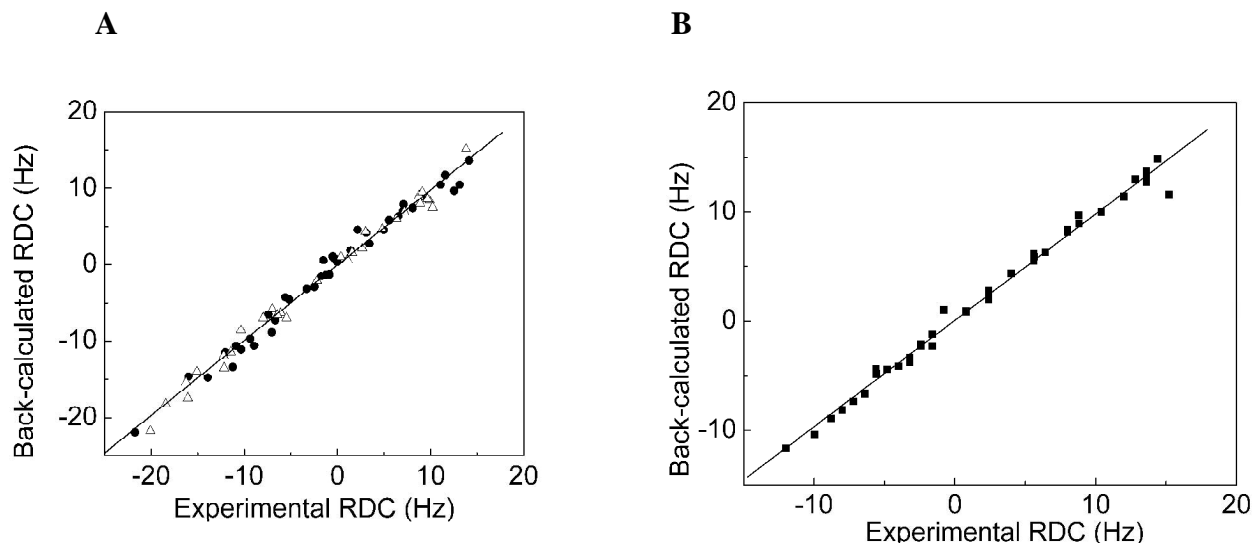


Figure 3S. Illustrates the fitting of experimental RDCs versus back-calculated RDCs from the refined Mystic structure. (A) Corresponds to the refinement of Mystic using compressed (●) and stretched (△) gel methods; (B) corresponds to the refinement of Mystic with 5mM halothane using compressed gel method.

IV. ^{15}N R_1 , R_2 , and NOE of Mystic in the absence and presence of 10 mM halothane

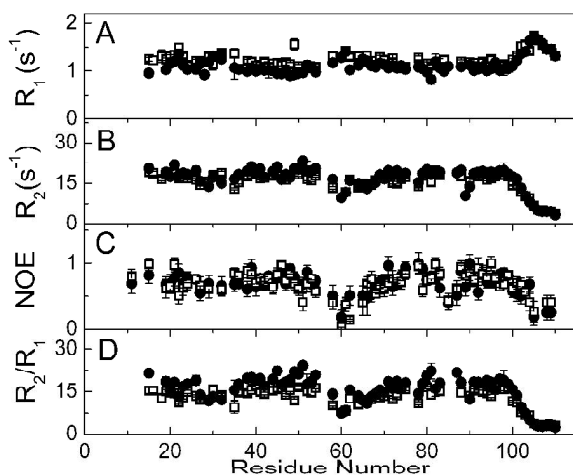


Figure 4S. ^{15}N backbone dynamics of Mystic in the absence (□) and presence (●) of 10 mM halothane as measured by: (A) Longitudinal relaxation rate, R_1 ; (B) Transverse relaxation rate, R_2 ; (C) ^{15}N - ^1H NOE; and (D) R_2/R_1 ratio plotted against residue number. Slightly increase in R_2/R_1 ratio suggested a small modification of global isotropic correlation time, τ_m , from 12.1 ns to 13.5 ns.

V. Residues involving in motion on the μ s-ms timescale

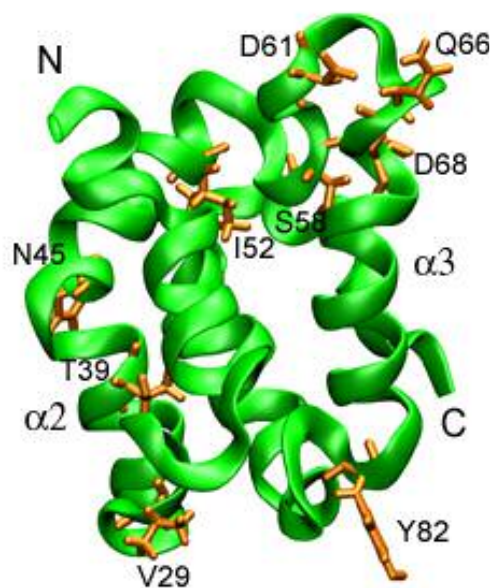


Figure 5S. Mystic residues involving in motion on the μ s-ms timescale are labeled and highlighted in orange color. In the loop connecting $\alpha 2$ and $\alpha 3$, residues D61 and Q66 are oriented upward, while residues S58 and D68 are oriented downward.

Table 1S. NH RDC data of Mystic aligned using compressed gel method at 800 MHz. Note that only residues in helical region are included.

Num1	Atom1	Num2	Atom2	RDCexptal	RDCBack	Diff.
15	N	15	HN	-9.98000		
18	N	18	HN	-13.9200	-14.7501	0.8301
19	N	19	HN	-11.2400	-13.3721	2.1321
20	N	20	HN	-15.9900	-14.6104	1.3796
21	N	21	HN	-10.9000	-10.5947	0.3053
35	N	35	HN	-8.9400	-10.5935	1.6535
36	N	36	HN	-9.3600	-9.6791	0.3191
38	N	38	HN	-7.4100	-6.5353	0.8747
39	N	39	HN	-7.0500	-8.8532	1.8032
40	N	40	HN	14.1300	13.6345	0.4955
41	N	41	HN	-12.0400	-11.4634	0.5766
45	N	45	HN	9.0000	8.9117	0.0883
46	N	46	HN	2.1600	4.5699	2.4099
47	N	47	HN	12.5400	9.6586	2.8814
48	N	48	HN	-1.7500	-1.5195	0.2305
49	N	49	HN	7.0900	7.8746	0.7846
51	N	51	HN	-5.6100	-4.2479	1.3621
52	N	52	HN	-0.0200	0.3525	0.3725
54	N	54	HN	8.0900	7.4228	0.6672
68	N	68	HN	-1.5000	0.5658	2.0658
69	N	69	HN	11.5800	11.7211	0.1411
70	N	70	HN	-0.3200	0.8328	1.1528
71	N	71	HN	11.0600	10.4422	0.6178
72	N	72	HN	13.1300	10.4532	2.6768
73	N	73	HN	-1.2700	-1.3419	0.0719
75	N	75	HN	4.9800	4.5384	0.4416
80	N	80	HN	6.5400	6.3403	0.1997
81	N	81	HN	-3.3000	-3.1426	0.1574
87	N	87	HN	5.5400	5.7912	0.2512
88	N	88	HN	3.4300	2.7592	0.6708
90	N	90	HN	7.0000	6.9517	0.0483
92	N	92	HN	-2.4600	-2.8831	0.4231
93	N	93	HN	-0.5100	1.0797	1.5897
94	N	94	HN	-0.8600	-1.2599	0.3999
95	N	95	HN	-10.3300	-11.0818	0.7518
96	N	96	HN	-5.1800	-4.5551	0.6249
97	N	97	HN	3.0900	4.1856	1.0956
98	N	98	HN	-6.6900	-7.2445	0.5545
100	N	100	HN	1.4200	1.8946	0.4746

Table 2S. NH RDC data of Mystic aligned using stretched charged gel method at 800 MHz. Note that only residues in helical region are included.

Num1	Atom1	Num2	Atom2	RDCexptal	RDCBack	Diff.
18	N	18	HN	6.3300	5.9529	0.3771
19	N	19	HN	2.6700	2.1168	0.5532
20	N	20	HN	13.8100	15.1401	1.3301
21	N	21	HN	8.7600	9.0253	0.2653
35	N	35	HN	-11.4400	-11.4265	0.0135
36	N	36	HN	1.0900	0.6687	0.4213
38	N	38	HN	9.1200	9.4888	0.3688
39	N	39	HN	7.1900	6.9373	0.2527
40	N	40	HN	-7.0000	-5.7890	1.2110
45	N	45	HN	9.9100	8.3776	1.5324
46	N	46	HN	-10.3500	-8.5434	1.8066
47	N	47	HN	-12.2200	-11.9024	0.3176
48	N	48	HN	4.8000	4.5459	0.2541
51	N	51	HN	4.8100	4.6259	0.1841
52	N	52	HN	1.5800	1.5658	0.0142
53	N	53	HN	-16.2500	-15.4064	0.8436
67	N	67	HN	8.8900	8.0114	0.8786
68	N	68	HN	3.0300	4.2929	1.2629
69	N	69	HN	-15.0900	-13.9689	1.1211
70	N	70	HN	0.3700	1.0171	0.6471
72	N	72	HN	10.2200	7.4917	2.7283
73	N	73	HN	-16.0600	-17.4570	1.3970
75	N	75	HN	-20.0800	-21.7369	1.6569
80	N	80	HN	-6.0900	-6.3148	0.2248
81	N	81	HN	-12.1700	-13.5094	1.3394
88	N	88	HN	-5.4800	-6.9908	1.5108
92	N	92	HN	9.6700	8.6117	1.0583
93	N	93	HN	-7.9700	-6.9781	0.9919
95	N	95	HN	-6.4500	-6.5795	0.1295
97	N	97	HN	-18.4300	-18.1890	0.2410
100	N	100	HN	-2.2000	-2.1091	0.0909

Table 3S. NH RDC data of Mystic with 5mM halothane aligned using compressed gel method at 800 MHz. Note that only residues in helical region are included.

Num1	Atom1	Num2	Atom2	RDCexptal	RDCBack	Diff.
15	N	15	HN	-9.9800	-10.380	0.3958
16	N	16	HN	-7.2100	-7.3570	0.1473
20	N	20	HN	-12.0100	-11.620	0.3875
21	N	21	HN	-8.8000	-8.9250	0.1250
36	N	36	HN	-6.4100	-6.6710	0.2614
38	N	38	HN	-3.2000	-3.7940	0.5936
39	N	39	HN	-4.0000	-4.1310	0.1309
40	N	40	HN	5.6000	5.5490	0.0510
41	N	41	HN	-8.0000	-8.1420	0.1419
45	N	45	HN	5.6100	5.8730	0.2625
46	N	46	HN	8.8000	9.7120	0.9122
47	N	47	HN	13.6100	12.760	0.8507
48	N	48	HN	13.6000	13.760	0.1583
49	N	49	HN	4.0100	4.3660	0.3566
52	N	52	HN	13.6100	13.440	0.1735
53	N	53	HN	-1.6000	-2.2820	0.6819
54	N	54	HN	10.4000	10.020	0.3837
68	N	68	HN	-5.5700	-4.8520	0.7176
69	N	69	HN	14.4000	14.850	0.4454
70	N	70	HN	2.4000	2.7970	0.3972
71	N	71	HN	15.2000	11.590	3.6070
73	N	73	HN	-1.6000	-1.201	0.3990
75	N	75	HN	8.0100	8.3620	0.3524
80	N	80	HN	5.6000	6.1680	0.5678
81	N	81	HN	0.8000	0.9037	0.1037
87	N	87	HN	12.8100	12.980	0.1749
88	N	88	HN	-2.4100	-2.1470	0.2626
92	N	92	HN	-3.2000	-3.3510	0.1513
93	N	93	HN	-0.8000	1.0440	1.8440
94	N	94	HN	2.4000	1.9470	0.4533
96	N	96	HN	-4.8000	-4.4160	0.3845
97	N	97	HN	8.0100	8.1460	0.1365
98	N	98	HN	12.0000	11.400	0.6005
100	N	100	HN	2.4000	2.3060	0.0941

Reference

1. Foster, R., and C. A. Fyfe. 1969. Chapter 1 Nuclear magnetic resonance of organic charge-transfer complexes. *Progress in Nuclear Magnetic Resonance Spectroscopy* 4:1.